PROCEEDINGS OF SCIENCE

Dense QC_2D. What's up with that?!?

Simon Hands,[a] **Seyong Kim,**[b] **Dale Lawlor,**[c,*] **Andrew Lee-Mitchell**[c,d] **and Jon-Ivar Skullerud**[c,e]

[a] *Department of Mathematical Sciences, University of Liverpool,Liverpool,L69 3BX,UK*
[b] *Department of Physics, Sejong University,Seoul 143–147,KR*
[c] *Department of Theoretical Physics, National University of Ireland Maynooth,Maynooth,Kildare,IE*
[d] *Department of Electronic Engineering, National University of Ireland Maynooth,Maynooth,Kildare,IE*
[e] *Hamilton Institute, National University of Ireland Maynooth,Maynooth,Kildare,IE*
E-mail: simon.hands@liverpool.ac.uk, skim@sejong.ac.kr, dalel487@thphys.nuim.ie, andrew.leemitchell.2021@mumail.ie, jonivar@thphys.nuim.ie

We present recent updates and results from QC_2D (Two Colour QCD) simulations at non-zero baryon density, including progress towards determining the speed of sound.

The 41st International Symposium on Lattice Field Theory (LATTICE2024)
28 July - 3 August 2024
Liverpool, UK

*Speaker

PoS(LATTICE2024)165

1. Introduction

Lattice simulations of QCD (Quantum Chromodynamics) at finite density are complicated by the complex fermion action inhibiting importance sampling. Fortunately, there are several QCD-like theories such as QC_2D [1–11], isospin QCD [12–14] or imaginary chemical potential studies which give insights into the behaviour of real QCD. Other lattice approaches are summarised nicely in [15]. This work focuses on QC_2D (Two Colour QCD) where we replace the $SU(3)$ gauge theory with an $SU(2)$ one. This does not exhibit a complex action problem for an even number of quark flavours[1].

Once one has settled on how best to simulate at finite density, the next thing to decide on is the best probe to study the finite density régime. An overview of non-lattice studies of dense QCD matter can be found in [17], but one popular method of exploring the QCD EoS (equation of state) is to look at how the speed of sound

$$C_s^2 = \frac{\partial P}{\partial \varepsilon} \tag{1}$$

behaves as density increases. Whilst it has been predicted from perturbation that C_s^2 approaches the conformal limit $\frac{1}{3}$ from below recent non-perturbative results [8, 10, 12], perturbative studies [17] and astronomical observations [18–21] appear to indicate otherwise. At the other end of the scale recent work in relativistic hydrodynamics suggest that there is an upper bound on C_s^2 from the shear viscosity [22].

This work has two objectives. To calculate the QC_2D speed of sound on a finer lattice than previously studied [8–10] and to consider a larger number of diquark sources aj at smaller values to get better control over the diquark source extrapolation.

2. Scale Setting and Beta Functions

Calculating C_s^2 requires evaluating the pressure P and energy density which shall be discussed further in section 3. In this work we determine the energy density via

$$\varepsilon = T_{\mu\mu} + 3P \tag{2}$$

$$T_{\mu\mu} = T^g_{\mu\mu} + T^q_{\mu\mu} \tag{3}$$

Both $T^g_{\mu\mu}$ and $T^q_{\mu\mu}$ require renormalisation by the beta functions which shall be discussed in subsections 2.1 and 2.2.

The beta functions in previous works [3–5] were derived using the Karsch coefficients, which requires anisotropic lattices (see the first three rows of table 1). For this work we instead determined β–κ pairs that lie on the line of constant physics $\frac{m_\pi}{m_\rho} \sim 0.81$. This requires multiple rounds of scale setting as seen in table 1.

2.1 Scale Setting: Mass Tuning

Firstly, for a chosen β we make an educated guess for what κ will give the correct mass ratio. We then produce $\sim$ 500 trajectories (saving every 5th configuration). As a non-physical theory there

[1] See [16] for a proof

are no physical quantities that we can compare with to conduct scale setting. Instead we calculate the *pion* (pseudoscalar) and *rho* (vector) correlators, fit to

$$C(\tau) = C_0 \cosh\left(M\left(\tau - \frac{N_\tau}{2}\right)\right) \tag{4}$$

and extracting the mass in lattice units as $am = |M|$. If after taking the pion and rho mass ratio we lie on the desired line of constant physics we can continue producing more configurations to improve statistics and prepare to evaluate the lattice spacing.

2.2 Scale Setting: Lattice Spacing

We determine the lattice spacing a from the Cornell form of the SQP (Static Quark Potential)

$$aV(r) = -\frac{N_c^2 - 1}{N_c}\frac{\alpha_s}{r} + a^2\sigma r + aV_0 \tag{5}$$

where α_s denotes the QCD running coupling and $\sigma = (440\,\text{MeV})^2$ the string tension. Previous works by our group have extracted the SQP by evaluating and fitting to Wilson loops. However, Wilson loops require path finding algorithms to evaluate and the cost scales poorly with the lattice volume. This work instead uses Wilson *lines*

$$W(\vec{x} - \vec{y}, t) = \text{Tr}\left(U(\vec{x}, t)U^\dagger(\vec{y}, t)\right) \tag{6}$$

and

$$U(\vec{x}, t) = \prod_{j=t}^{t+l} U_4(\vec{x}, j) \tag{7}$$

where $0 < l < \frac{N_t}{2}$ to extract the SQP. Results in preparation indicate that the Wilson loop and Wilson line (fixed to Coulomb gauge) results agree within 2σ, but with less computation needed.

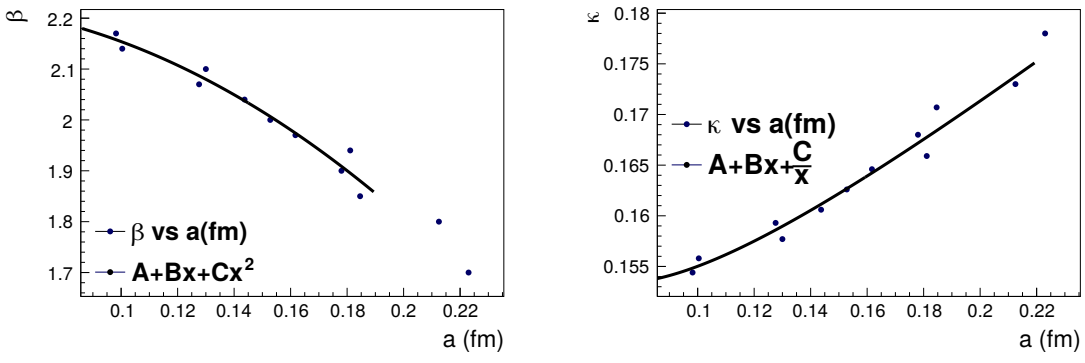

(a) β vs a and quadratic fit.

(b) κ vs a and its fit.

Figure 1: Fits to extract beta functions.

β	κ	n_{cfg}	a (fm)	$\pm$	$\frac{m_\pi}{m_\rho}$	$\pm$	am_π
1.7	*0.1780*		*0.223*	*0.004*	*0.779*	*0.004*	*0.79*
1.9	*0.1680*		*0.187*	*0.004*	*0.805*	*0.009*	*0.645*
2.1	*0.1577*		0.130	0.0004	*0.810*	*0.004*	*0.446*
1.80	0.1730	1019	0.2125	0.0019	0.811	0.008	0.731
1.85	0.1707	277	0.1846	0.0015	0.828	0.021	0.684
1.97	0.1646	175	0.1617	0.0008	0.829	0.027	0.546
2.00	0.1626	268	0.1528	0.0006	0.799	0.022	0.562
2.04	0.1606	293	0.1437	0.0004	0.799	0.018	0.520
2.14	0.1558	106	0.1004	0.0007	0.801	0.045	0.410
2.17	0.1544	100	0.0741	0.0016	0.813	0.009	0.381

Table 1: β and κ values on line of constant physics $\frac{m_\pi}{m_\rho} = 0.81$. Italicised values are from earlier works.

β	κ	$\frac{\partial\beta}{\partial a}$	$\pm$	$\frac{\partial\kappa}{\partial a}$	$\pm$	Remarks
1.9	0.1680	-2.71	0.16	0.197	0.16	Karsch Coefficients in [5]
1.9	0.1680	-2.86	0.08	0.195	0.32	This work
2.1	0.1577	-2.85	0.10	0.152	0.32	This work

Table 2: Beta functions as extracted from figure 1. The first two lines correspond to the coarse lattice used in [1–7]. The last line are the values for the fine lattice used in this work.

2.3 Remarks

In table 2 we also present the beta functions corresponding to the coarse lattice used in [1–7]. The values we obtained here are consistent with those obtained using the Karsch coefficients, which gives us confidence that the beta functions for the fine lattice used here are sane. This scale setting approach is different to that used in [8–10] where instead the spacing is tuned such that at $N_t = 10$ at zero density the temperature $T = 200\,\text{MeV}$.

3. Simulation Details and Thermodynamic Observables

We are using an unimproved Wilson fermion and gauge action for this simulation. At non-zero chemical potential the superfluid phase contains low-lying eigenmodes, so we introduce a *diquark source* term $aj = 0.01, 0.015, 0.02, 0.03$ to lift these modes making the simulation feasible and extrapolate to $j = 0$. All the results shown here are from the *fine* lattice where $\beta = 2.1$ and $\kappa = 0.1577$. This gives a spacing of $a = 0.130\,\text{fm}$. Our quark masses are tuned so that they lie on the line of constant physics $\frac{m_\pi}{m_\rho} = 0.81$ discussed in section 2.

We primarily choose chemical potential $a\mu_q$ at intervals of 0.050, with increased resolution around the onset chemical potential $\mu_0 = \frac{m_\pi}{2} = 0.223$. Beyond $a\mu_q \sim 0.75$ lattice artefacts render the results unreliable. If we consider the $\frac{\mu_q}{m_\pi}$ axis we can explore higher chemical potentials than previous studies relative to the onset and critical chemical potentials due to the finer lattice spacing.

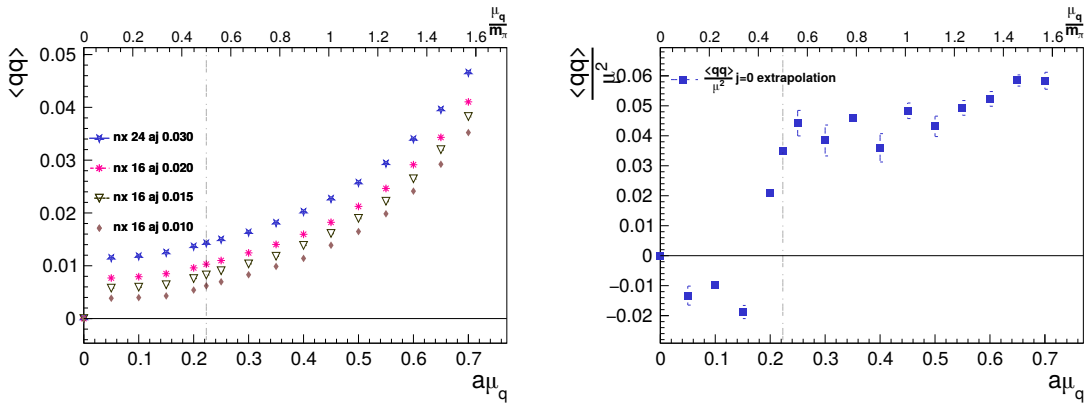

(a) Diquark condensate at $aj = 0.30, 0.20, 0.15, 0.10$.

(b) Diquark condensate extrapolated to $aj = 0.0$ and normalised by μ_q^2.

Figure 2: Diquark Condensate

3.1 Simulation Code

The new gauge ensembles and scale setting data were produced over six weeks using the code in [23]. The major improvements over the original [1–7] code are a mixed precision conjugate gradient, changing to the RANLUX [24] generator, improved hybrid OpenMP/MPI support on CPU based machines and a CUDA port. These ensembles were generated using the CUDA version of the code.

The scale setting and analysis codes can also be found at [25] alongside the data used in the speed of sound analysis at [26]. The gauge configurations are not available on Zenodo but can be provided on request.

3.2 Diquark Condensate

The diquark $\langle qq \rangle$ states are effectively the baryons of QC_2D. Unlike real QCD these consist of only two quarks so are bosonic (the quarks themselves remain fermionic). The diquark condensate is strongly dependent on the diquark source so needs to be extrapolated to $aj = 0$. We do this by fitting

$$\langle qq \rangle = C_0 + C_1 j^{C_2} \tag{8}$$

χPT (Chiral Perturbation Theory) predicts that $C_2 = \frac{1}{3}$ near onset. However at high densities this value is clearly violated. Above the onset chemical potential $\mu_0 \sim \frac{m_\pi}{2}$ the diquark condensate takes on a non-zero value indicating the transition from a hadronic phase to a superfluid phase.

3.3 Quark Number Density and Pressure

The pressure is determined by integrating the quark number density with respect to μ_q. Unlike $\langle qq \rangle$ it is only weakly dependent on the diquark source and is extrapolated to $aj = 0$ using a linear fit. We also require the non-interacting lattice SB (Stefan-Boltzmann) results to mitigate IR and UV artefacts in the pressure. The continuum and lattice SB forms for non-interacting fermions can be

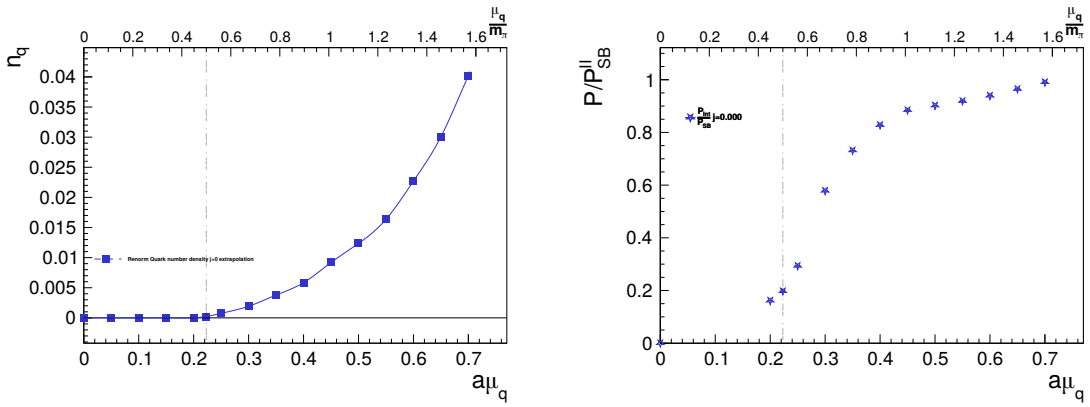

(a) Zero Extrapolated quark number density corrected by $\frac{n_q^{\text{Cont}}}{n_q^{\text{Lat}}}$.

(b) Pressure vs μ_q corrected using Scheme II.

Figure 3: Number density and pressure corrected by their SB values.

found in [7] and [1] respectively.

$$n_q^{\text{Lat}} = \frac{4N_f N_c}{N_s^3 N_t} \sum_k \frac{i \sin \tilde{k}_0 \left[\sum_i \cos k_i - \frac{1}{2\kappa} \right]}{\left[\frac{1}{2\kappa} - \sum_\nu \cos \tilde{k}_\nu \right]^2 + \sum_\nu \sin^2 \tilde{k}_\nu} \tag{9}$$

As was discussed in [4, 7] in order to evaluate n_q^{Lat} one must consider a larger spatial volume than the one actually used. For this work, $4N_s$ was considered. We interpolate the quark number density using a cubic spline. We have two schemes to correct for lattice artefacts int the pressure as described in [4, 7]

$$\text{Scheme II}: \frac{P}{P_{\text{SB}}}(\mu_q) = \frac{1}{P_{\text{Cont}}(\mu_q)} \int_0^{\mu_q} \frac{n_q^{\text{Cont}}}{n_q^{\text{Lat}}}(\mu')\, n_q(\mu')\, d\mu' \tag{10}$$

where the continuum SB pressure is given by

$$P_{\text{Cont}} = \frac{N_f N_c}{12\pi^2} \left(\mu_q^4 + 2\pi^2 \mu_q^2 T^2 + \frac{7\pi^4}{15} T^4 \right) \tag{11}$$

Both the earlier results and this work indicate that Scheme II best approximates the SB result at higher density. Thus we shall use it to evaluate C_s^2.

3.4 Trace Anomaly

As mentioned in section 1 we will derive ε from the trace anomaly. From equation (3) we see that the trace anomaly consists of a gluonic and a fermionic component given by

$$T^g_{\mu\mu} = -\frac{3a}{N_c} \frac{\partial \beta}{\partial a} \text{Re} \left(\text{Tr}\, U_{ij} + \text{Tr}\, U_{i0} \right) \tag{12}$$

$$T^q_{\mu\mu} = -a \frac{\partial \kappa}{\partial a} \kappa^{-1} \left(4N_f N_c - \langle \bar{\psi}\psi \rangle \right) \tag{13}$$

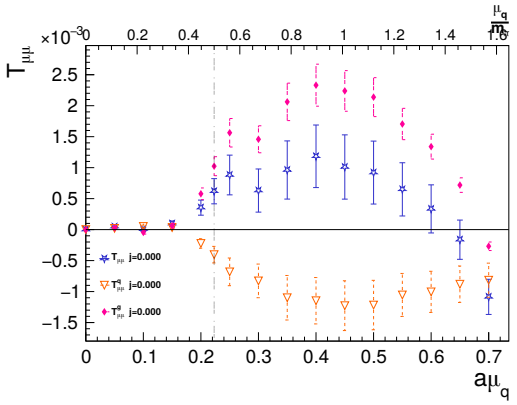

Figure 4: Trace Anomaly

The beta functions $\frac{\partial\beta}{\partial a}$ and $\frac{\partial\kappa}{\partial a}$ were evaluated in section 2. Thus all that is left to do is evaluate the plaquette sum and $\langle\bar{\psi}\psi\rangle$ as seen in figure 5. The plaquette sum and $\langle\bar{\psi}\psi\rangle$ depend weakly on the diquark source so a linear fit was again used for the zero diquark source extrapolation. We then subtract the $\mu = 0$ values to obtain figure 5. We can then calculate the full trace anomaly and use equation (2) to extract the energy density as seen in figure 6b.

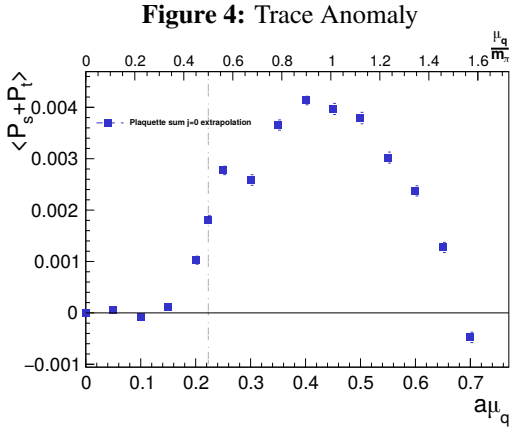

(a) Subtracted and extrapolated plaquette sum.

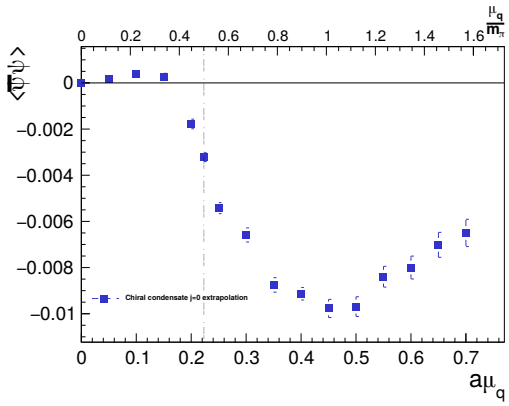

(b) Subtracted and extrapolated chiral condensate.

Figure 5: Zero subtracted and diquark extrapolated plaquette sum and chiral condensate.

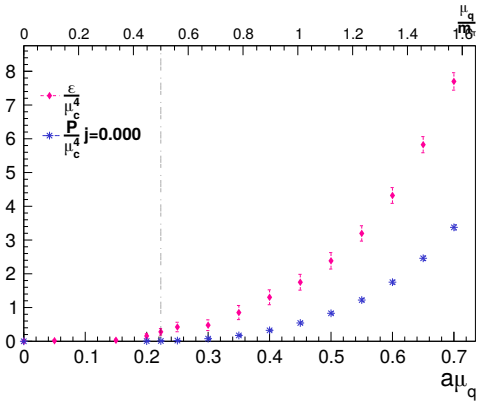

(a) P and ε normalised by the onset chemical potential $\mu_c = m_\pi$.

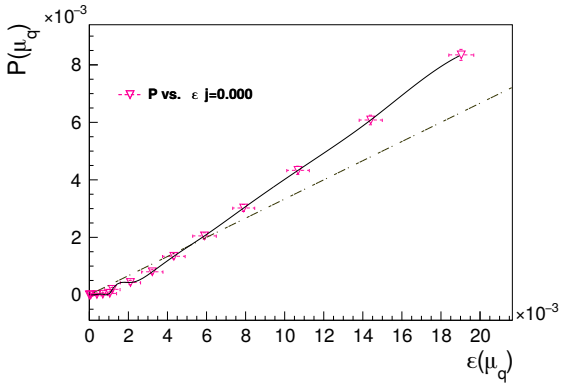

(b) Pressure versus energy density at $aj = 0$. Black line is a cubic spline interpolation. Dashed line is the conformal limit.

Figure 6: Pressure and Energy Density

3.5 Speed of sound

Finally, we have all we need to evaluate the speed of sound. We do this by taking the symmetric derivative of P with respect to ε. The results in figure 7 are consistent with other recent QC_2D works [8–10]. There is a sharp increase above at the onset chemical potential and C_s^2 clearly breaches the conformal limit. This behaviour has also been observed in isospin QCD simulations. Similarly to [8–10] we observe that C_s^2 stops behaving like the χPT prediction at higher densities and remains well below the bound predicted by relativistic hydrodynamics in [22].

4. Discussions

Whilst these early results are promising, there is still more work to do. Measurements have been taken for every trajectory, meaning there may be autocorrelations present. The lower diquark source runs were conducted at relatively small lattice spatial volume $L_s = 16^3$. The error analysis has been crude thus-far. Errors in measured observables were boot-strapped rather than jackknifed with multiple elements removed and errors from fits are currently read off of the fitting function.

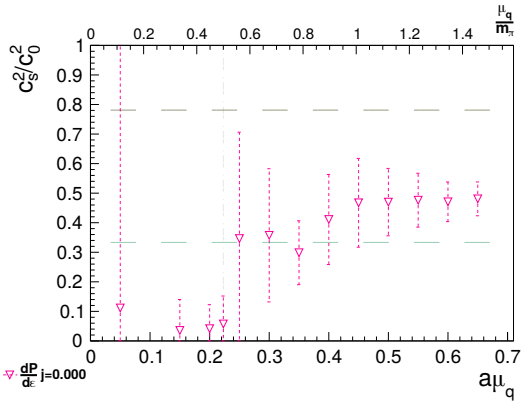

Figure 7: Speed of sound. Upper region denotes area forbidden by relativistic hydrodynamics in [22].

Moving forward we intend on running all diquark sources at a larger volume with ~ 1000 configurations. A run at $aj = 0.005$ is also underway after upgrades to the HMC integrator. Lastly, work is underway to implement a Symanzik Improved fermion action to allow further exploration of finer lattice spacings.

Acknowledgements

This work used the DiRAC Extreme Scaling service (Tursa) at the University of Edinburgh, managed by the Edinburgh Parallel Computing Centre on behalf of the STFC DiRAC HPC Facility (www.dirac.ac.uk). The DiRAC service at Edinburgh was funded by BEIS, UKRI and STFC capital funding and STFC operations grants.

Simulations were also performed on the Luxembourg national supercomputer MeluXina. Access was provided through the ICHEC National Service mechanism. The authors acknowledge the LuxProvide and ICHEC teams for their expert support.

Acronyms

EoS equation of state

HMC hybrid Monte Carlo

QC_2D Two Colour QCD

QCD Quantum Chromodynamics

SB Stefan-Boltzmann

SQP Static Quark Potential

χPT Chiral Perturbation Theory

References

[1] S. Hands, S. Kim and J.-I. Skullerud, *Deconfinement in dense 2-color QCD*, *Eur. Phys. J. C* **48** (2006) 193 [hep-lat/0604004].

[2] S. Hands, S. Kim and J.-I. Skullerud, *A Quarkyonic Phase in Dense Two Color Matter?*, *Phys. Rev. D* **81** (2010) 091502 [1001.1682].

[3] T. Boz, S. Cotter, L. Fister, D. Mehta and J.-I. Skullerud, *Phase transitions and gluodynamics in 2-colour matter at high density*, *Eur. Phys. J. A* **49** (2013) 87 [1303.3223].

[4] S. Cotter, P. Giudice, S. Hands and J.-I. Skullerud, *Towards the phase diagram of dense two-color matter*, *Phys. Rev. D* **87** (2013) 034507 [1210.4496].

[5] S. Cotter, *Non-perturbative determination of Karsch Coefficients in 2 Colour QCD*, philosophiæ doctor, National University of Ireland Maynooth, 2015.

[6] T. Boz, *Quark and Gluon Propagation in Two-Colour Quantum Chromodynamics at Finite Density*, philosophiæ doctor, National University of Ireland Maynooth, 2018.

[7] T. Boz, P. Giudice, S. Hands and J.-I. Skullerud, *Dense two-color QCD towards continuum and chiral limits*, *Phys. Rev. D* **101** (2020) 074506 [1912.10975].

[8] K. Iida, E. Itou, K. Murakami and D. Suenaga, *Lattice study on finite density QC_2D towards zero temperature*, *JHEP* **10** (2024) 022 [2405.20566].

[9] E. Itou and K. Iida, *Speed of sound exceeding the conformal bound in dense 2-color QCD*, *PoS* **LATTICE2023** (2024) 111 [2311.15259].

[10] K. Iida and E. Itou, *Velocity of sound beyond the high-density relativistic limit from lattice simulation of dense two-color QCD*, *PTEP* **2022** (2022) 111B01 [2207.01253].

[11] A. Begun, V.G. Bornyakov, V.A. Goy, A. Nakamura and R.N. Rogalyov, *Study of two color QCD on large lattices*, *Phys. Rev. D* **105** (2022) 114505 [2203.04909].

[12] B.B. Brandt, F. Cuteri and G. Endrődi, *Equation of state and speed of sound of isospin-asymmetric QCD on the lattice*, *JHEP* **07** (2023) 055 [2212.14016].

[13] B.B. Brandt, G. Endrődi and S. Schmalzbauer, *QCD phase diagram for nonzero isospin-asymmetry*, *Phys. Rev. D* **97** (2018) 054514 [1712.08190].

[14] B.B. Brandt, G. Endrődi, E.S. Fraga, M. Hippert, J. Schaffner-Bielich and S. Schmalzbauer, *New class of compact stars: Pion stars*, *Phys. Rev. D* **98** (2018) 094510 [1802.06685].

[15] K. Nagata, *Finite-density lattice QCD and sign problem: Current status and open problems*, *Prog. Part. Nucl. Phys.* **127** (2022) 103991 [2108.12423].

[16] S. Hands, I. Montvay, S. Morrison, M. Oevers, L. Scorzato and J. Skullerud, *Numerical study of dense adjoint matter in two color QCD*, *Eur. Phys. J. C* **17** (2000) 285 [hep-lat/0006018].

[17] H. Koehn et al., *An overview of existing and new nuclear and astrophysical constraints on the equation of state of neutron-rich dense matter*, 2402.04172.

[18] T.E. Riley et al., *A NICER View of PSR J0030+0451: Millisecond Pulsar Parameter Estimation*, *Astrophys. J. Lett.* **887** (2019) L21 [1912.05702].

[19] M.C. Miller et al., *PSR J0030+0451 Mass and Radius from NICER Data and Implications for the Properties of Neutron Star Matter*, *Astrophys. J. Lett.* **887** (2019) L24 [1912.05705].

[20] LIGO Scientific, Virgo collaboration, *GW170817: Measurements of neutron star radii and equation of state*, *Phys. Rev. Lett.* **121** (2018) 161101 [1805.11581].

[21] LIGO Scientific, Virgo collaboration, *GW170817: Observation of Gravitational Waves from a Binary Neutron Star Inspiral*, *Phys. Rev. Lett.* **119** (2017) 161101 [1710.05832].

[22] M. Hippert, J. Noronha and P. Romatschke, *Upper Bound on the Speed of Sound in Nuclear Matter from Transport*, 2402.14085.

[23] D. Lawlor, S. Hands, S. Kim and J.-I. Skullerud, *su2hmc*, July 2024. 10.5281/zenodo.12910604.

[24] Lüscher, Martin, *A Portable high quality random number generator for lattice field theory simulations*, *Comput. Phys. Commun.* **79** (1994) 100 [hep-lat/9309020].

[25] J.-I. Skullerud and D. Lawlor, *QC_2D Analysis Suite*, Dec. 2024. 10.5281/zenodo.14503846.

[26] D. Lawlor and J.-I. Skullerud, *Dense QC_2D. What's up with that?!? The dataset.*, Nov. 2024. 10.5281/zenodo.14201453.

PoS(LATTICE2024)165